

# Embeddings and delays as derived from quantification of recurrence plots

Joseph P. Zbilut<sup>1</sup>

*Department of Physiology, Rush Medical College, Rush-Presbyterian-St. Luke's Medical Center,  
1653 W. Congress, Chicago, IL 60612, USA*

and

Charles L. Webber Jr.

*Department of Physiology, Loyola University Medical Center, 2160 South First Avenue, Maywood, IL 60153, USA*

Received 13 August 1992; revised manuscript received 14 September 1992; accepted for publication 18 September 1992  
Communicated by A.R. Bishop

Recurrence plots have been advocated as a useful diagnostic tool for the assessment of dynamical time series. We extend the usefulness of this tool by quantifying certain features of these plots which may be helpful in determining embeddings and delays.

## 1. Introduction

A persistent problem in the dynamical analysis of experimental time series has been the diagnosis of assumptions of autonomy with respect to adequate length of relatively high quality data. Eckmann, Ollifson Kamphorst and Ruelle [1] demonstrated that recurrence plots are a useful diagnostic tool in this respect.

Basically their idea is that, after choosing an embedding, dots are plotted  $(i, j)$  on an  $N \times N$  array whenever point  $x(j)$  is sufficiently close to point  $x(i)$  of an orbit for a given embedding and delay. Their definition for sufficiently close includes a nearest neighbor classification used for calculation of Lyapunov exponents. Examination of these plots for dynamical systems revealed the existence of short line segments parallel to the diagonal of the recurrence plot, which are related to the inverse of the largest positive Lyapunov exponent. Random data do not demonstrate these short line segments. These plots have proved useful, especially in the case of biolog-

ical data where stationarity of long time series are rather difficult to obtain [2–4].

Although these plots can provide a qualitative assessment of systems, as recurrences and short line segments increase, the visual inspection becomes complicated. To this end we calculated both the number of recurrences, as well as the number of these short, deterministic line segments, which resulted in unexpected findings regarding embeddings and delays.

## 2. Quantification

To provide a measure of the short line segments, we first calculate the recurrences in the following manner: the distances between each of the time-ordered sequence of vectors in  $\mathbb{R}^n$ ,  $x(i)$ , and each of the successive vectors forward in time,  $x(j)$ , is calculated to create a square matrix. Graphically, the horizontal axis of the square matrix represents the time index,  $x(i)$ , whereas the vertical axis represents the time shift,  $x(j)$ . A dot is then placed in the array,  $(i, j)$ , if  $x(j)$  is sufficiently close to  $x(i)$ . Here suf-

<sup>1</sup> Author for correspondence.

ficiently close means that  $x(j)$  falls within a ball of radius  $r$  centered at  $x(i)$ , where  $r$  is fixed (in this we differ from the Eckmann et al. algorithm) – see ref. [2] for specifics. In practice we fix  $r$  values as small as possible (typically not greater than 10% of the normalized mean distance of the first embedding) relative to the noise level. We express the number of these dots as a percent of the upper diagonal of the  $N \times N$  matrix, excluding the identity line. The number of recurrent points which constitute a line segment, defined as two or more points adjacent to each other, and parallel to the diagonal are then determined. This value is expressed as a percentage of recurrent points.

There is some debate regarding the appropriate norm for calculation of distances with respect to questions of accuracy of the original data. For the present work we used the Euclidean norm. For additional perspectives see refs. [2,5,6].

### 3. Results with known dynamics

In order to understand the behavior of percent recurrence and percent line segments, we analyzed the results for 2000 points (after transients) for increasing embeddings and delays of: (i) the Lorenz equations [7]

$$\frac{dx_1}{dt}(t) = \sigma[x_2(t) - x_1(t)],$$

$$\frac{dx_2}{dt}(t) = -x_1(t)x_3(t) + rx_1(t) - x_2(t),$$

$$\frac{dx_3}{dt}(t) = x_1(t)x_2(t) - bx_3(t), \quad (1)$$

for the usually fixed values of  $\sigma=10$ ,  $b=\frac{8}{3}$ ,  $r=28$ , and time step of 0.01 (fractal dimension=2.6 [8]); (ii) the Mackey–Glass differential delay equations [9]

$$\frac{dX}{dt} = \frac{aX(t-s)}{1 + [X(t-s)]^c} - bX(t), \quad (2)$$

for  $a=0.1$ ,  $b=0.2$ ,  $s=10$ , and  $c=17$  (fractal dimension=2.13 [10]); (iii) the Hénon map [11]

$$x_1(n+1) = 1 - ax_1(n)^2 + x_2(n),$$

$$x_2(n+1) = bx_1(n), \quad (3)$$

for  $a=1.4$ , and  $b=0.3$  (fractal dimension=1.26 [8]); and (iv) a sequence of uniformly distributed pseudo-random numbers on the unit interval, generated by a PC workstation.

Figures 1, 2 demonstrate the results for increasing embedding and delays for the Lorenz and Mackey–Glass equations. As can be seen for both equations, the recurrences begin to increase noticeably for an embedding of three, with clear relative maxima (at a delay of 17 in the Lorenz example, and 12 in the Mackey–Glass example) in subsequent embeddings. These results are accounted for by the gradual topological unfolding of the attractor.

The results are disappointing for the Hénon mapping (fig. 3)). There is no clear maximum, although there are some fluctuations, and they are somewhat similar to the results found for the random example (fig. 4).

When we calculate for the line segments, however, the unfoldings become much more distinct. For the Lorenz (fig. 5) and Mackey–Glass equations (fig.

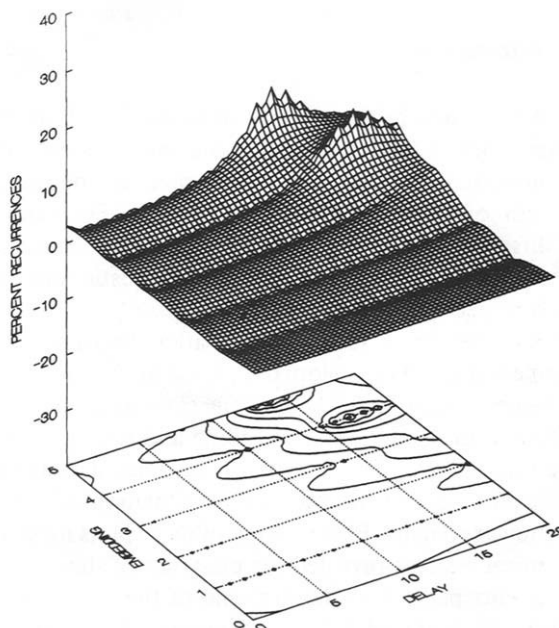


Fig. 1. Smoothed response surface (using an inverse least squares algorithm) for recurrence values for the Lorenz equations versus increasing embeddings and delays. Values are based on 2000 data points. Note the minimal increase in recurrences for an embedding of 3 and delay > 15.

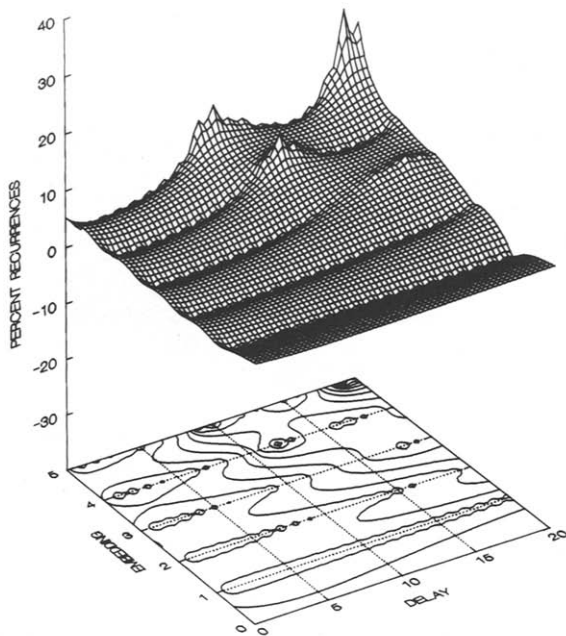


Fig. 2. Smoothed response surface for recurrences for the Mackey-Glass equation. Note that the increase in recurrences at embedding 3, delay 17 is not continuous with the fourth embedding.

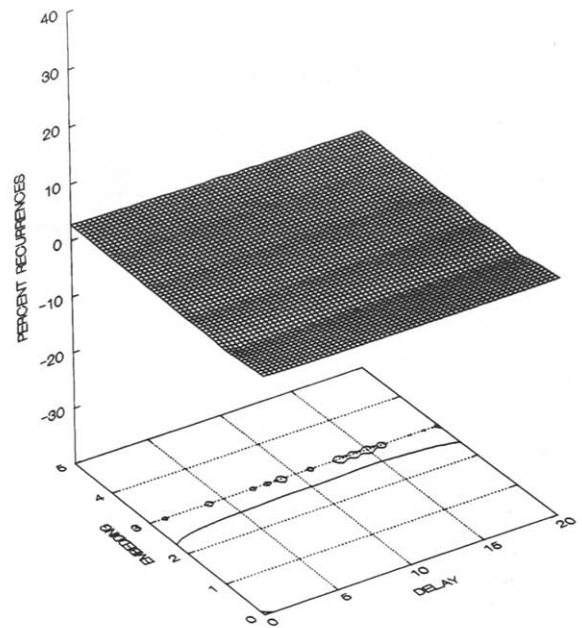


Fig. 4. Recurrence surface for 2000 points of uniformly distributed pseudorandom data on the unit interval.

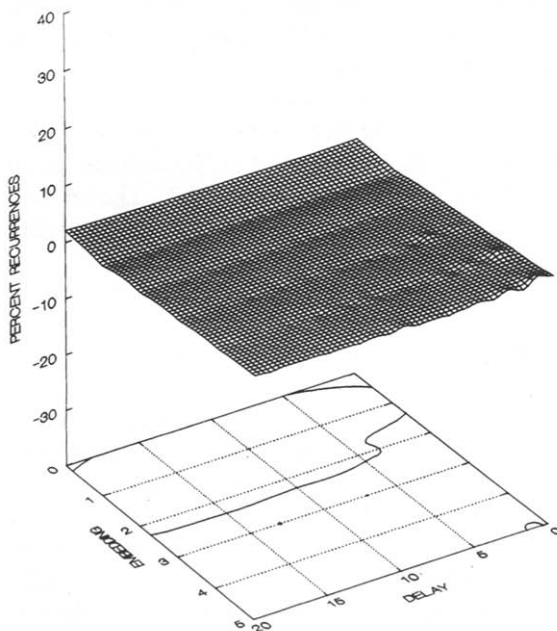


Fig. 3. Smoothed response surface for recurrences for the Hénon map.

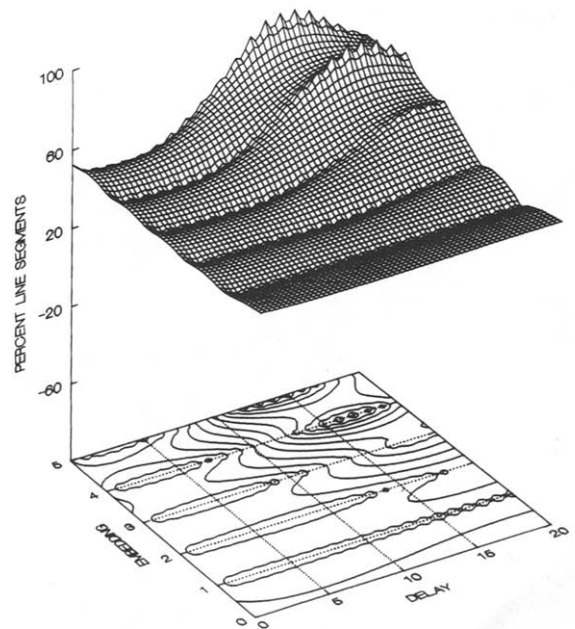


Fig. 5. Percent line segments for the Lorenz equations.

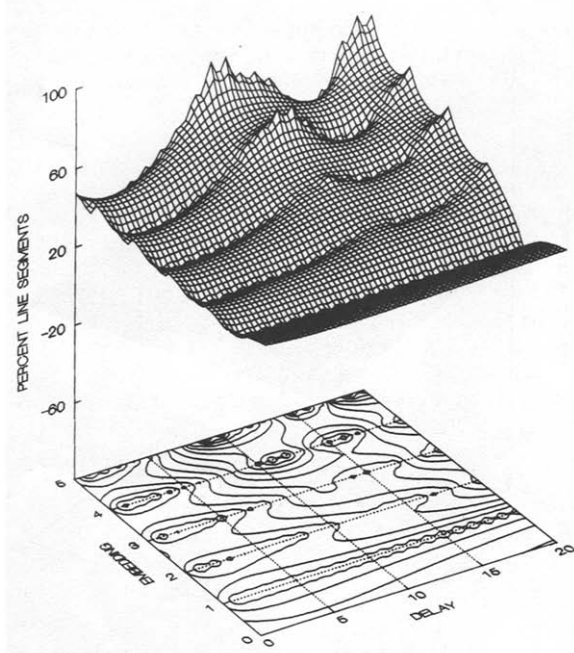


Fig. 6. Percent line segments for the Mackey-Glass equations. Note that the increases seen in embedding 3, delay 12, continue in subsequent embeddings. Compare with fig. 2.

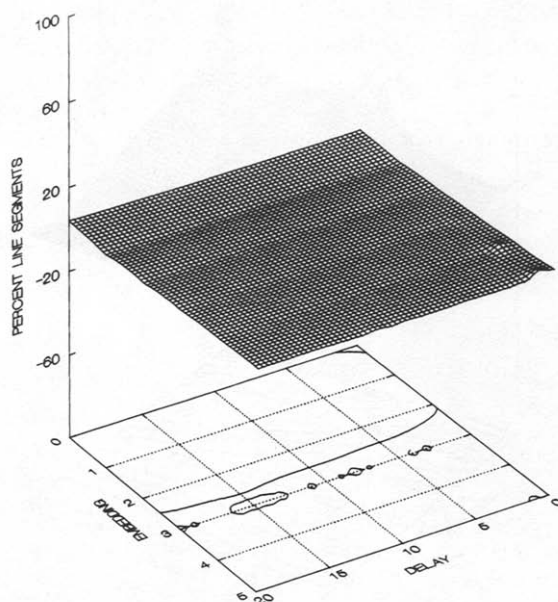


Fig. 8. Percent line segments for the uniform random data.

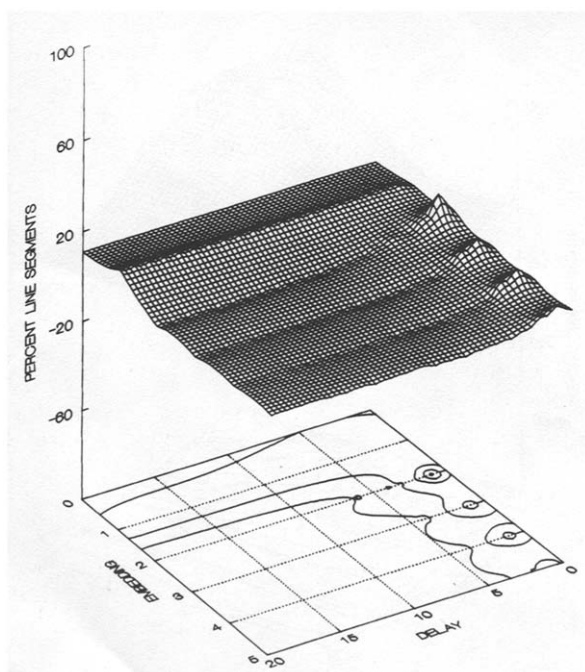


Fig. 7. Percent line segments for the Hénon mapping.

6) we obtain clear peaks at an early embedding of 3, at a delay of 17 for the Lorenz, and 12 for the Mackey-Glass example. We note that these are the first minima we obtained for the autocorrelation function for these data lengths.

The results for the Hénon mapping are much more striking with the unfolding clearly occurring at an embedding of 2 and delay of 1 (fig. 7). The random data, on the other hand, remain relatively constant, with a very gradual increase, at a delay of 1.

#### 4. Conclusions

We have demonstrated that quantification of recurrences and line segments from recurrence plots can be an excellent tool for the investigation of dynamical time series, and can provide information about embeddings, delays, and the likelihood of the existence of a low-dimensional object. We stress the usual cautions regarding spurious results derived from time series which are too short, very noisy, or are not stationary [12,13], and note that evaluation of the recurrence plot itself is designed for exami-

nation of these assumptions. Nonetheless, a demonstration of "unfoldings" of recurrences and/or line segments may be of some interest in itself, apart from an evaluation of scaling behavior in the entire range of distances, in that it may provide confirmation that a seemingly random process is really part of a dynamical system.

### Acknowledgement

We wish to thank Gottfried Mayer-Kress and David Ruelle for useful discussions and comments.

### References

- [1] J.-P. Eckmann, S. Ollifson Kamphorst and D. Ruelle, *Europhys. Lett.* 4 (1987) 973.
- [2] J.P. Zbilut, M. Koebbe, H. Loebbe and G. Mayer-Kress, in: *Proc. IEEE Computers in cardiology 1990*, eds. A. Murray and K.L. Ripley (IEEE Computer Soc. Press, Silver Spring, MD, 1991) p. 263.
- [3] J.P. Zbilut, in: *Springer series in synergetics*, Vol. 55. *Rhythms in physiological systems*, eds. H. Haken and H.P. Koepchen (Springer, Berlin, 1991) p. 139.
- [4] C.L. Webber Jr., in: *Springer series in synergetics*, Vol. 55. *Rhythms in physiological systems*, ed. H. Haken and H.P. Koepchen (Springer, Berlin, 1991) p. 177.
- [5] N.A. Gershenfeld, *Physica D* 55 (1992) 135.
- [6] H. Baruchli, *Lecture notes in mathematics*, Vol. 503 (Springer, Berlin, 1976) p. 235.
- [7] E.N. Lorenz, *J. Atmos. Sci.* 20 (1963) 130.
- [8] P. Bergé, Y. Pomeau and C. Vidal, *Order within chaos* (Wiley, New York, 1984).
- [9] M.C. Mackey and L. Glass, *Science* 197 (1977) 287.
- [10] J.D. Farmer, *Physica D* 4 (1982) 366.
- [11] M. Hénon, *Commun. Math. Phys.* 50 (1976) 69.
- [12] J.-P. Eckmann and D. Ruelle, *Physica D* 56 (1992) 185.
- [13] P. Grassberger, T. Schreiber and C. Schaffrath, *Int. J. Bifurcation Chaos* 1 (1991) 521.